Borrower's Name	Alex Noguerola	Org. or A.U.	1744	Phone	305-5686
Serial Number	08/845,660	Date of Request	6/11/99	Date Needed By	6/16/99

Please Attach Copy of Abstract, Citation, Or Bibliography. If Available Please Provide Complete Citation. Only One Request Per Form.

Author/Editor:	See attached sheet. Date of Publn.
Journal/Book Title:	
Article Title:	Journal of the Chemical Society, Perkins Trans. 2
Volume (Issue):	
Pages:	
Year of Publication:	
Publisher:	
Remarks:	

COMPLETED

STIC Use Only B TECH Micro

Accession Number: 25361

LIBRARY ACTION	LC		NAL		NIH		NLM		NBS		PTO		OTHER	
	1st	2nd	1st	2nd	1st	2nd	1st	2nd	1st	2nd	1st	2nd	1st	2nd
Local Attempts														
Date														
Initials														
Results														
Examnr. Called														
Page Count														
Money Spent														

Provided By: Source and Date

Ordered From: Source and Date

Remarks/Comments
- 1st & 2nd denotes times taken to a library
- FX - Means Faxed to us
- O/N - Under NLM=Overnight Service

L2 ANSWER 9 OF 45 CAPLUS COPYRIGHT 1999 ACS
AN 1996:718838 CAPLUS
DN 126:89748
TI Design and synthesis of flavin-conjugated **peptides** and assembly on a gold **electrode**
AU Sakamoto, Seiji; Aoyagi, Haruhiko; Nakashima, Naotoshi; Mihara, Hisakazu
CS Dep. Applied Chem., Fac. Eng., Nagasaki Univ., Nagasaki, 852, Japan
SO J. Chem. Soc., Perkin Trans. 2 (1996), (11), 2319-2326
CODEN: JCPKBH; ISSN: 0300-9580
PB Royal Society of Chemistry
DT Journal
LA English
CC 34-3 (Amino Acids, Peptides, and Proteins)
Section cross-reference(s): 22, 72
AB Flavin-conjugated **peptides** composed of one or two amphiphilic .alpha.-**helix** segments have been designed and synthesized. 7-Acetyl-10-methylisoalloxazine (Fla) as a model flavin has been introduced on the side chain of Cys at the 6th, 7th or 8th position of each .alpha.-**helical** 14-peptide. A CD study in aq. soln. revealed that the position of Fla on the peptide strongly influenced the peptide secondary structure. Addnl., CD spectra indicated that the Fla in the **peptides** was oriented in a different manner depending on the position when the peptide took on the .alpha.-**helix** structure. Furthermore, the flavin-conjugated **peptides** have been adsorbed on a gold surface through the sulfide linkage, as a basic study for peptidyl devices in the future. By the use of FLA as an electrochem. probe, we examd. properties of the peptide assembled on the gold **electrode**. The cyclic voltammetry measurements revealed that the functional group, Fla, was redox-active on the **electrode** and the peptide bound on the surface in a monolayer. Moreover, the flavin-conjugated peptide could mediate the electron transfer from the **electrode** to Fe(CN)63- ion or cytochrome c in a vector manner. The redox-active probe, Fla, has been demonstrated to provide significant information about the assembly and function of the .alpha.-**helix** **peptides** on the gold **electrode** surface by electrochem. measurements.
ST flavin conjugated peptide prepn property; conformation flavin conjugated peptide; fluorescence flavin conjugated peptide; cyclic voltammetry flavin conjugated peptide; redox potential flavin conjugated peptide
IT Conformation
Cyclic voltammetry
Fluorescence

Design and synthesis of flavin-conjugated peptides and assembly on a gold electrode

Seiji Sakamoto,†[a] Haruhiko Aoyagi,[a] Naotoshi Nakashima[a] and Hisakazu Mihara*[b]

[a] *Department of Applied Chemistry, Faculty of Engineering, Nagasaki University, Nagasaki 852, Japan*
[b] *Department of Bioengineering, Faculty of Bioscience and Biotechnology, Tokyo Institute of Technology, Midori-ku, Yokohama 226, Japan*

Flavin-conjugated peptides composed of one or two amphiphilic α-helix segments have been designed and synthesized. 7-Acetyl-10-methylisoalloxazine (Fla) as a model flavin has been introduced on the side chain of Cys at the 6th, 7th or 8th position of each α-helical 14-peptide. A CD study in aqueous solution revealed that the position of Fla on the peptide strongly influenced the peptide secondary structure. Additionally, CD spectra indicated that the Fla in the peptides was oriented in a different manner depending on the position when the peptide took on the α-helix structure. Furthermore, the flavin-conjugated peptides have been adsorbed on a gold surface through the sulfide linkage, as a basic study for peptidyl devices in the future. By the use of Fla as an electrochemical probe, we examined properties of the peptide assembled on the gold electrode. The cyclic voltammetry measurements revealed that the functional group, Fla, was redox-active on the electrode and the peptide bound on the surface in a monolayer. Moreover, the flavin-conjugated peptide could mediate the electron transfer from the electrode to $Fe(CN)_6^{3-}$ ion or cytochrome c in a vector manner. The redox-active probe, Fla, has been demonstrated to provide significant information about the assembly and function of the α-helix peptides on the gold electrode surface by electrochemical measurements.

The high selectivity and efficiency of natural proteins arise from their regulation of the positions of functional groups and chromophores in the defined 3D structure. Along with this aspect, much attention has been focused on the organization of functionalities in the 3D structure by *de novo* design methods. Considerable efforts in the design of artificial proteins have been devoted to the construction of the 3D structures of polypeptides[1–5] and the introduction of functional chromophores.[6–11] For example, DeGrado, Dutton and co-workers reported the design and synthesis of artificial polypeptides which have iron protoporphyrin IX in a 4α-helix bundle structure.[8] We also demonstrated that the organization of oriented functionalized chromophores, such as pyrene,[9] quinone, viologen, ruthenium trisbipyridine complex,[10a] flavin and porphyrins,[10b–d] could be accomplished by the use of designed peptide scaffolds.

On the other hand, in order to use functionalized artificial polypeptides as chemical sensors and electronic devices, methods will be required for the assembly of peptides with regulated orientation on material surfaces such as metal electrodes. Several rational methods for the alignment of organic compounds, such as Langmuir–Blodgett (LB) films and self-assembled monolayers (SAMs), have been investigated and utilized for the surface design. In particular, SAMs utilizing the high affinity of a thiol group for gold or silver, have some advantages such as stability and simplicity of preparation. Additionally, SAMs can control the orientation of molecular units. By the use of these properties, several SAMs of functionalized molecules such as resorcin[4]arene,[12] cyclodextrin,[13] DNA,[14] porphyrin[15] and other photo-active molecules[16] were constructed on a gold surface and investigated for the design of chemical and electrochemical sensors. However, so far, there are only a few examples of studies of peptide assembly on a gold surface.[17] Recently, Whitesell and Chang demonstrated the construction of an oriented α-helical peptide monolayer of polyalanine and polyphenylalanine on a gold surface through the S–Au bond.[17a] In their report, they investigated the secondary structure, orientation and thickness of the assembly of the peptide on a gold surface by Fourier transform infrared (FT-IR) techniques. However, because the peptide layer was built by the polymerization of *N*-carboxyanhydrides of amino acids, this method is not generally applicable for the *de novo* designed polypeptides which have designed amino acid sequences, 3D structures and functionalized chromophores. Thus, development of a method for constructing the assembly of functional polypeptides is required for peptidyl devices in future.

As a basic study for the assembly of a functionalized polypeptide, we attempted the adsorption of a designed α-helical peptide through a sulfide linkage on a gold electrode surface. To examine the properties of the peptide fixed on the gold surface by a conventional electrochemical method, we introduced a functionalized chromophore, 7-acetyl-10-methylisoalloxazine (Fla)[10d,18] as a model flavin, into an α-helix segment. It is known that flavin itself is redox-active on an electrode, although many biological molecules are redox-inactive. So far, direct immobilization of flavin on an electrode by physical[19–21] and chemical adsorption methods[22,23] and by an LB method[24] has been extensively studied. Thus, we utilized a flavin as an electrochemical probe to examine the properties of peptides bound on a gold electrode surface. In the present study, we designed and synthesized flavin-conjugated peptides composed of one or two amphiphilic α-helix segments (Fig. 1). The flavin-conjugated peptides were adsorbed on a gold electrode surface through a sulfide linkage. By the use of cyclic voltammetry techniques, we examined the packing mode, the occupied area and other electrochemical properties of the peptides assembled on the electrode surface.

† Present address: Department of Bioengineering, Faculty of Bioscience and Biotechnology, Tokyo Institute of Technology, Midori-ku, Yokohama 226, Japan.

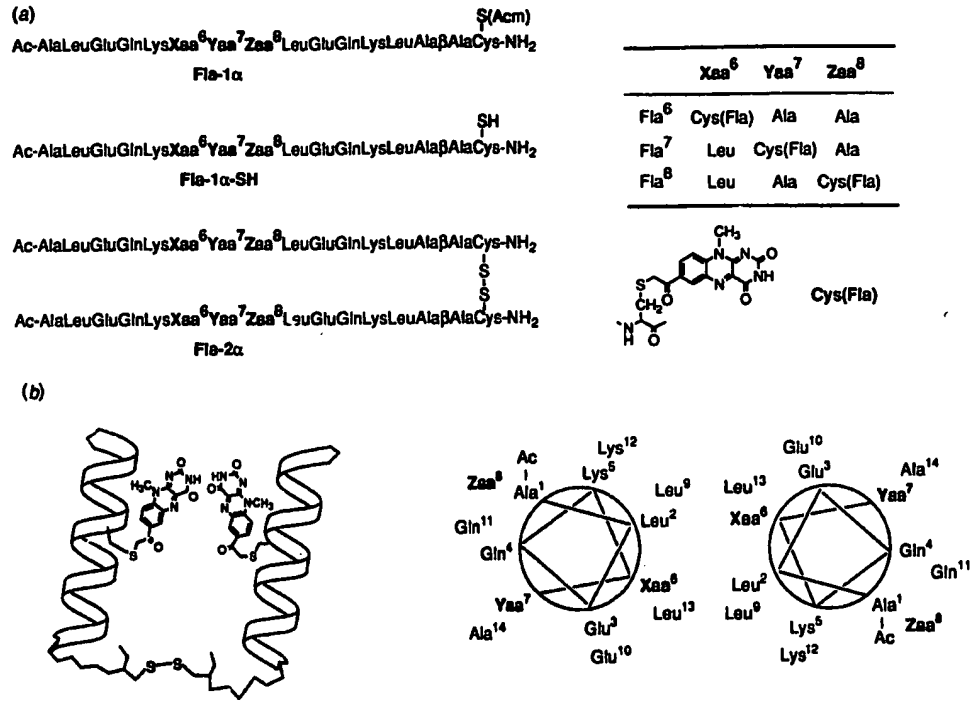

Fig. 1 Structure of the flavin-conjugated peptides. Fla-1α, Fla-1α-SH and Fla-2α. (*a*) Amino acid sequence of the Fla-1α, Fla-1α-SH and Fla-2α and structure of Cys(Fla). (*b*) Illustration of two-α-helix peptide structures and helix wheel drawings of the two 14-peptides in coiled-coil form.

Results and discussion

Design and synthesis

The 14-peptide was designed to take an amphiphilic α-helical structure employing Ala, Gln, Glu, Leu and Lys residues which tend to form an α-helix (Fig. 1). The Leu residues were deployed on the α-helix segment in the same manner as hydrophobic amino acids in coiled-coil proteins to define the packing mode between the two α-helix segments.[25] Coiled-coil sequences in proteins consist of heptad repeats containing two characteristic hydrophobic positions, *i.e.* (-a-b-c-d-e-f-g-)$_n$ in which the a and d residues are hydrophobic ones such as Leu. The 14-peptide consists of two repeats of the sequence c-d-e-f-g-a-b where the a and d residues are Leu, f is hydrophilic Gln, b and c are Ala, e is Glu and g is Lys. The Glu of e and Lys of g positions were arranged to be able to form salt bridges between the two α-helix segments. To increase the stability of the α-helix structure, the *N*-terminal amino and *C*-terminal carboxy group were acetylated and amidated, respectively. Though the 14-peptide is not long enough to form a coiled-coil structure, 14 residues in length would be sufficient to stabilize an α-helix structure (four turns in the α-helix at the maximum).[9a] To construct a parallel two α-helix structure, the two segments were dimerized by the disulfide linkage of Cys[16] residues with a flexible spacer of β-Ala. To evaluate the differences of α-helicity depending on the positions of flavin on the peptide scaffold, Fla was introduced on the side chain of Cys at the 6th, 7th or 8th position in each peptide instead of Leu or Ala. When the peptides take an α-helix structure, each Fla should exist under different environments on the amphiphilic α-helical structure. That is, it is expected that Fla in the Fla^6-1α is on the hydrophobic face of the amphiphilic α-helix. On the other hand, Fla in the Fla^7- and Fla^8-1α are on the hydrophilic face.

The peptide synthesis was carried out manually by solid-phase synthesis using an Fmoc-strategy (Fmoc, 9-fluorenylmethyloxycarbonyl).[26] The acetyl 16-peptides were synthesized by stepwise elongation of Fmoc-amino acids on the 4-(2',4'-dimethoxyphenylaminomethyl)phenoxy resin (NH-SAL resin)[27] with different protecting groups on Cys [Cys at the 6th, 7th or 8th position was protected with the trityl (Trt) group and Cys at the 16th position was protected with the acetamidomethyl (Acm) group]. Removal of the protecting groups except for the Acm group and cleavage from the resin were carried out with trifluoroacetic acid (TFA). After HPLC purification of each acetyl 16-peptide, 7α-bromoacetyl-10-methylisoalloxazine was reacted with the Cys^6, Cys^7 or Cys^8 side chain of the partially protected [Cys(Acm)[16]] peptides.[10d,18] The flavin-conjugated 16-peptides (Fla^6-1α, Fla^7-1α and Fla^8-1α) were purified by gel filtration to remove unreacted or hydrolysed flavin derivatives. Fla-1α-peptides were treated with $AgBF_4$ in the presence of anisole as a scavenger to remove the Acm protecting group of Cys at the 16th position.[28] After purification by gel filtration, Acm-deprotected peptides (Fla-1α-SH) were obtained without considerable amounts of by-products (>95% purity on HPLC). These Fla^6, Fla^7 and Fla^8-1α-SH were used for adsorption on a gold electrode. Subsequently, each Fla-1α-SH was dimerized by air oxidation to give the Fla-2α peptide. The Fla-2α peptides were purified by gel filtration to remove the unreacted 1α-peptides. All the peptides and intermediates synthesized were identified by amino acid analysis, matrix assisted laser desorption ionization time-of-flight mass spectrometry (TOFMS) and fast atom bombardment mass spectrometry (FABMS). To determine apparent molecular weights of the peptides in aqueous solution, the peptide samples (2.0×10^{-5} mol dm^{-3}) were passed through a Pharmacia Superdex 75HR column (10 × 300 mm, 5.0×10^{-2} mol dm^{-3} phosphate buffer, pH 7.0) calibrated with protein molecular weight markers. The peptides gave a slightly large apparent molecular weight (3200 and 6300 for 1α and 2α peptides, respectively) as compared to the theoretical one (2100 and 4000 for 1α and 2α peptides, respectively). It is reasonably considered that Fla-1α- and Fla-2α-peptides are in a monomeric form in buffer, because the peptides take a relatively extended conformation.

UV–VIS and fluorescence spectra

The Fla-1α-peptides showed UV–VIS spectra with three absorption maxima at 288–289, 350 and 430 nm in buffer. Similarly, UV–VIS spectra of the Fla-2α-peptides were composed of three absorption maxima at 286–288, 350 and 430 nm. Except for slight differences, all flavin-conjugated peptides showed similar absorption spectra to Fla with three absorption maxima at 282, 349 and 427 nm in buffer as reported by Kaiser *et al.*[18a] These results indicate that Fla is introduced into the peptide without unfavourable side-reactions.

Fluorescence spectra of the Fla-1α, Fla-2α peptides and Fla were also examined. The relative fluorescence intensities of peptides and Fla are listed in Table 1. Fluorescence emission peaks at 505 nm of all peptides in buffer were quenched in 6–10% intensities as compared to that of Fla. This is attributed to the flavin linked to the peptide with sulfur as reported by Kaiser *et al.*[18a,39] Hence, flavin was demonstrated to be on the Cys side chain. The relative fluorescence intensities of peptides in trifluoroethanol (TFE) were increased as compared with those in buffer, but diminished as compared with that of Fla. Moreover, the Fla in each peptide showed a fluorescence emission with different intensity depending on its position in the peptide scaffold. Presumably, this fact indicates that the Fla in each peptide exists under different environments on the amphiphilic α-helix structure.

CD study

The CD spectra of the synthetic peptides in buffer and TFE solutions were examined and the results are shown in Fig. 2. In buffer, all the Fla-1α peptides showed low α-helicity (13–15%) calculated from an ellipticity at 222 nm (−4000 to −4600 deg cm^2 $dmol^{-1}$) (Table 2).[30] The 16-peptide is not long enough to form stable hydrogen bonds for α-helix structure formation in aqueous solution.[9a] On the other hand, the α-helicity of each Fla-2α in buffer was higher than that of the corresponding Fla-1α. However, the flavin position in the peptide differently affects the α-helix conformation (Fla^6-2α, 20%; Fla^7-2α, 28%; Fla^8-2α, 46%). It is considered that the stabilization of the α-helix is mainly attained by the intramolecular interaction between the hydrophobic face of the amphiphilic α-helical segments.[1–10] Because Fla^6-2α has only six Leu residues, two residues less than Fla^7- and Fla^8-2α, the α-helicity was lower than that of the others. It is noteworthy that Leu^6-2α, which is a non-Fla peptide, has 55% helicity in the buffer solution. Another possible factor is that the relatively large and hydrophilic Fla was introduced at the hydrophobic Leu^6 position in the 2α-helix structure. The hydrophobic interaction between the two α-helices of Fla^6-2α was disrupted by the introduced Fla group. When the α-helicity of Fla^7-2α is compared with that of Fla^8-2α, the former is lower than the latter. This result cannot be explained only by the hydrophobic effect between the two

Table 1 Relative fluorescence intensities of 7-acetyl-10-methylisoalloxazine and flavin-conjugated peptides[a]

Solvent	7-Acetyl-10-methyl-isoalloxazine (Fla)	Fla^6		Fla^7		Fla^8	
		1α	2α	1α	2α	1α	2α
Buffer	100	7.4	8.4	7.8	6.4	9.5	6.4
TFE	143	32.5	27.5	16.9	15.6	24.6	17.6

[a] Intensity of Fla in buffer taken as 100. Measured in 2.0×10^{-2} mol cm^{-3} Tris·HCl buffer, pH 7.4 or trifluoroethanol at the flavin concentration of 2.0×10^{-5} mol dm^{-3} at 25 °C; excitation 430 nm, emission 510 nm.

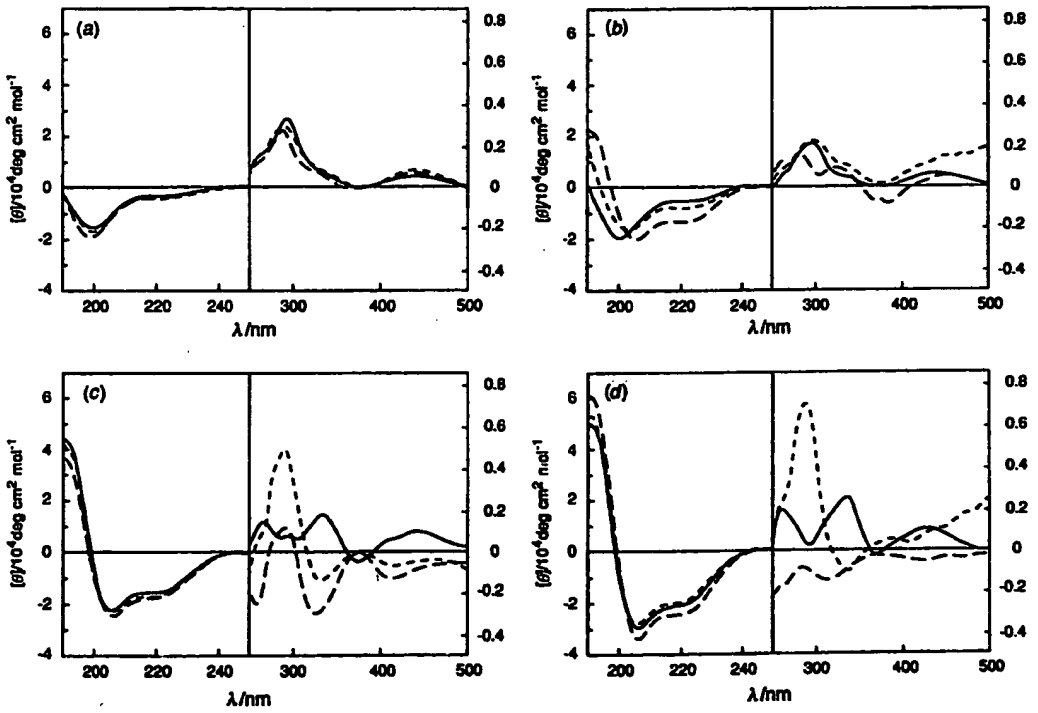

Fig. 2 CD spectra of Fla-1α-[(*a*) and (*b*)] and Fla-2α-peptides [(*c*) and (*d*)] in 2.0×10^{-2} mol dm^{-3} Tris·HCl buffer, pH 7.4 [(*a*) and (*c*)] and TFE [(*b*) and (*d*)]. (——) Fla^6-1α and 2α peptides; (-·-·-) Fla^7-1α and 2α peptides; (– – –) Fla^8-1α and 2α peptides. [*θ*] at the amide region is the mean residual weight ellipticity, and [*θ*] at the flavin absorption region is the molar ellipticity for Fla. [Fla-1α] = 2.0×10^{-5} mol dm^{-3}, [Fla-2α] = 1.0×10^{-5} mol dm^{-3}; 25 °C.

Table 2 α-Helix content (%) of Fla-1α- and Fla-2α-peptides[a]

Peptide	Solvent	
	Buffer	TFE
Fla[6]-1α	13	52
Fla[7]-1α	15	56
Fla[8]-1α	14	59
Leu[6]-1α	16	68
Fla[6]-2α	20	67
Fla[7]-2α	28	64
Fla[8]-2α	46	68
Leu[6]-2α	55	67

[a] The concentrations of 1α and 2α peptides were 2.0×10^{-5} mol dm^{-3} and 1.0×10^{-5} mol dm^{-3}, respectively.

α-helix segments. Flavin in some flavoproteins, such as glucose oxidase[31] and lipoamide dehydrogenase,[32] is known to form hydrogen bonds with the main chain amides. It is possible that such hydrogen bonds are differently formed and thus affect the α-helicity depending on the position of flavin on the peptide. Consequently, these results indicate that the position of Fla in the peptides influences the secondary structure of peptides in aqueous solution. On the other hand, all Fla-1α and Fla-2α peptides showed a typical α-helix CD pattern in TFE. TFE is known to be an α-helix forming solvent and affects the hydrophobic interaction between α-helical segments causing them to be separated.[25a] In TFE, all the peptides have similar potential to form an α-helix. Additionally, FT-IR spectra of Fla-1α-SH in cast films, which were prepared from TFE solution, exhibited narrow absorption peaks for the amide I and II bands; Fla[6]-1α-SH 1656 and 1547 cm^{-1}, Fla[7]-1α-SH 1651 and 1541 cm^{-1}, Fla[8]-1α-SH 1654 and 1544 cm^{-1} for amide I and II bands, respectively. These wavenumbers corresponding to amide I and II bands were characteristic for an α-helix rather than a random structure.[33]

Flavins on the Fla-1α peptides in buffer showed induced CD spectra at wavelengths corresponding to the UV spectra. Because Fla-1α peptides in buffer were almost in a random structure, flavins on Cys side chains were thought to move freely and not to be oriented in a particular position. However, flavins on the Fla-1α peptides in TFE showed different CD spectra depending on their positions. This result indicates that the flavin on each peptide is fixed in a particular orientation when the peptides are in an α-helix structure. The interaction between Fla and the peptide side chains in an α-helix structure may contribute to the different orientation of Fla. There were some differences among CD spectra in the flavin region of Fla-2α peptides in buffer. These differences were probably due to the distinct α-helicity of each peptide caused by the inter-helix hydrophobic interaction. In a similar manner to Fla-1α, flavins on the Fla-2α also showed different CD spectra in TFE. Consequently, these results suggested that flavins conjugated with peptides were arranged in different orientations depending on their positions when the peptides took an α-helix structure.

Modification of gold electrode with Fla-1α-SH

To adsorb the flavin-conjugated peptides on a gold surface through the sulfide linkage, a polished gold disk electrode was immersed in a solution of Fla-1α-SH (1.0×10^{-3} mol dm^{-3}) in TFE or water for 10 h at 25 °C. Because we thought that Fla-1α-SH was more easily adsorbed than Fla-1α, we used Fla-1α-SH for the modification of a gold electrode. Subsequently, to avoid the non-specific physical adsorption of peptides, the electrode was sonicated in TFE and water. Fla-1α-SH-modified electrodes which were obtained by immersion in aqueous solution almost completely blocked the direct electron transfer between the electrode and $Fe(CN)_6^{3-}$ in solution. This was detected by the blocking ability of the heterogeneous electron

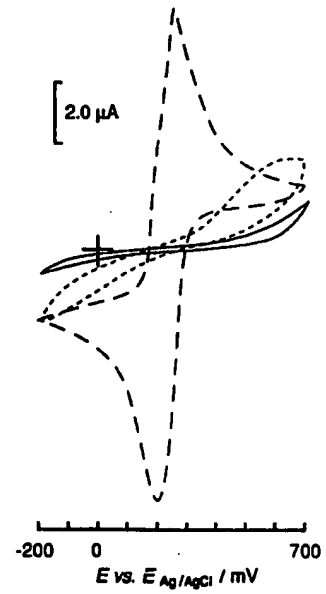

Fig. 3 Cyclic voltammograms for Fla[6]-1α-SH-modified gold electrode prepared in aqueous solution (——), Fla[6]-1α-SH modified gold electrode prepared in TFE solution (- - - - -) and bare gold (unmodified) electrode (– – –). Measured in 2.0×10^{-3} mol dm^{-3} $K_3[Fe(CN)_6]$–0.1 mol dm^{-3} phosphate buffer, pH 7.0 at 100 mV s^{-1} sweep rate at 25 °C.

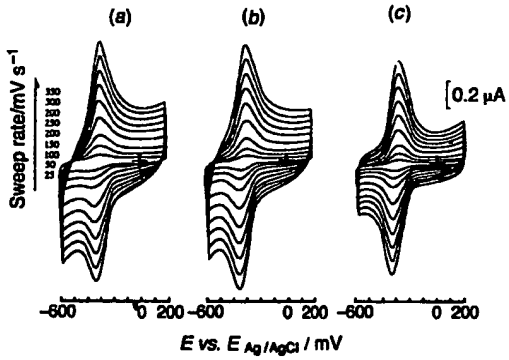

Fig. 4 Cyclic voltammograms for gold electrodes modified with the Fla-peptides in 0.1 mol dm^{-3} phosphate buffer, pH 7.0 at 25 °C; (*a*) Fla[6]-1α-SH, (*b*) Fla[7]-1α-SH, (*c*) Fla[8]-1α-SH

transfer between the peptide–gold electrode and $Fe(CN)_6^{3-}$ in solution (Fig. 3). On the other hand, when the peptides were adsorbed in TFE, a disordered submonolayer was obtained on the electrode, resulting in insufficient blocking of the electron transfer. In TFE, hydrophobic interaction between peptides is cancelled in adsorption processes, and disordered layers might be formed. In water, on the contrary, hydrophobic interaction between peptides is stronger than that in TFE, and peptides would be organized in a closely packed mode on the electrode surface. Thus, for cyclic voltammetry measurements, we used the modified electrode which was prepared in the aqueous solution of Fla-1α-SH.

Electrochemical characterization of modified electrodes

Fig. 4 shows typical cyclic voltammograms at various sweep rates obtained for Fla-1α-SH-modified gold electrodes in 0.1 mol dm^{-3} phosphate buffer, pH 7.0. Each Fla-1α-SH-modified electrode showed a well-defined redox peak at *ca.* −320 mV (*vs.* Ag/AgCl). The E° value of Fla was comparable to the reported

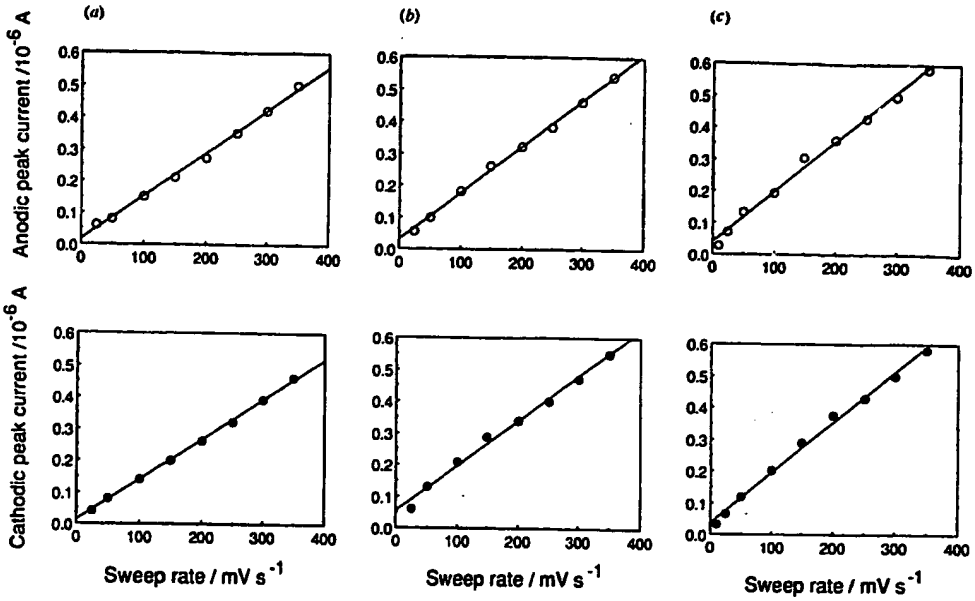

Fig. 5 Plots of anodic and cathodic peak currents as a function of the sweep rate for Fla-peptide modified electrodes in 0.1 mol dm^{-3} phosphate buffer, pH 7.0 at 25 °C; (*a*) Fla^6-1α-SH, (*b*) Fla^7-1α-SH, (*c*) Fla^8-1α-SH

Table 3 Redox potential and area occupied per Fla-1α-SH molecule bound on an electrode surface[a]

Peptide	Solvent for adsorption	Redox potential/mV	Adsorbed amount/10^{-11} mol cm^{-2}	Molecular occupied area/Å²
Fla^6-1α-SH	TFE	−323	4.0	420
	H_2O	−319	10.7	155
Fla^7-1α-SH	TFE	−322	6.0	280
	H_2O	−329	10.7	155
Fla^8-1α-SH	TFE	−320	4.0	420
	H_2O	−314	12.3	135

[a] Measured in 0.1 mol dm^{-3} phosphate buffer, pH 7.0, at 25 °C. Surface area of Au disk electrode was 2.01 mm^2; reference electrode was Ag/AgCl.

one (−300 mV *vs.* Ag/AgCl), which was measured in solution.[18a] Fig. 5 shows the plots of anodic and cathodic peak currents as a function of the sweep rate. The linearity of these plots indicates that the voltammetric responses arise from surface-bound molecules. These results demonstrate that the Fla-peptides are successfully immobilized and redox-active on the gold electrode. In addition to these results, values of anodic and cathodic peak currents were approximately equal, and the peak potentials were independent of the sweep rate, indicating that Fla-1α-SH on a gold electrode caused almost reversible redox reaction in the buffer solution.

Integration of the redox peak afforded an electro-active Fla-1α-SH coverage of 10.7–12.3 × 10^{-11} mol cm^{-2}, based on the surface area of the electrode (Table 3). The occupied area per peptide was 155, 155 and 135 Å², respectively, for Fla^6-, Fla^7- and Fla^8-1α-SH, respectively, which corresponded well to the theoretical area of the α-helical peptide adsorbed through the sulfide bond in the monolayer. Because FT-IR spectra of the Fla-1α-SH cast film were characteristic of an α-helix, Fla-1α-SH bound on the electrode might take an α-helix structure. The area occupied per Fla^8-1α-SH molecule was slightly lower than that of Fla^6- and Fla^7-1α-SH. As mentioned in the discussion on the CD spectra, the position of Fla in the peptides influences the secondary structure of peptides in aqueous solution. Therefore, the closer packing of Fla^8-1α-SH may be attributed to the difference in the secondary structure on the surface. In contrast, when a gold disk electrode was immersed in a solution of peptide in TFE, the peptides adsorbed at 4.0–6.0 × 10^{-11} mol cm^{-2}. In this case, the area occupied by the peptides varied from 280 to 420 Å², 1.8–3.1 times larger than those adsorbed in water. This result is consistent with incomplete blocking ability against the direct electron transfer from the electrode to $Fe(CN)_6^{3-}$ ion as described above. The peptides adsorbed in TFE were loosely packed on the gold surface. Therefore, it is concluded that the hydrophobic interaction between peptides is important for the peptide adsorption process on a gold surface with a sulfide linkage.

Catalytic reduction of $Fe(CN)_6^{3-}$ ion and cytochrome c by Fla-1α-SH-modified electrode

The ability of flavin to act as a redox-active coenzyme makes it possible to mediate the electron transfer from a two-electron reductant such as NADH to a one-electron oxidant such as haem-Fe^{III} in proteins. Hence, it is reasonable to expect that the flavin-conjugated peptides on the electrode play a role as a mediator for reduction of $Fe(CN)_6^{3-}$ ion or cytochrome c. Fig. 6 shows the cyclic voltammograms of Fla-1α-SH-modified electrodes in the presence of $Fe(CN)_6^{3-}$ ion in the range of 700 to −600 mV. As seen in Fig. 3, the direct electron transfer between $Fe(CN)_6^{3-}$ ion and the electrode was almost completely blocked by the peptide monolayer on the gold surface. Another notable CV result in the presence of $Fe(CN)_6^{3-}$ ion was the drastic enhancement in the peak at the reduction potential (around −330 mV) of Fla-1α-SH. This result is ascribed to the catalytic reduction of $Fe(CN)_6^{3-}$ ion in the bulk solution through the flavin on the peptide. That is, Fla-1α-SH on the electrode could mediate the electron transfer from the electrode to $Fe(CN)_6^{3-}$ ion in a vector manner.

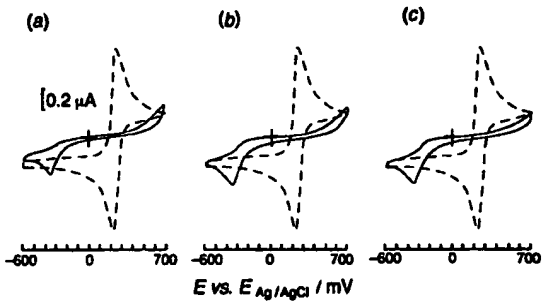

Fig. 6 Cyclic voltammograms for the gold electrodes modified with the flavin-conjugated peptides (——) and bare gold (unmodified) electrode (– – –) in 2.0×10^{-3} mol dm^{-3} $K_3[Fe(CN)_6]$–0.1 mol dm^{-3} phosphate buffer, pH 7.0 at 25 °C; (*a*) Fla^6-1α-SH, (*b*) Fla^7-1α-SH, (*c*) Fla^8-1α-SH. The sweep rate was 100 m V s^{-1}.

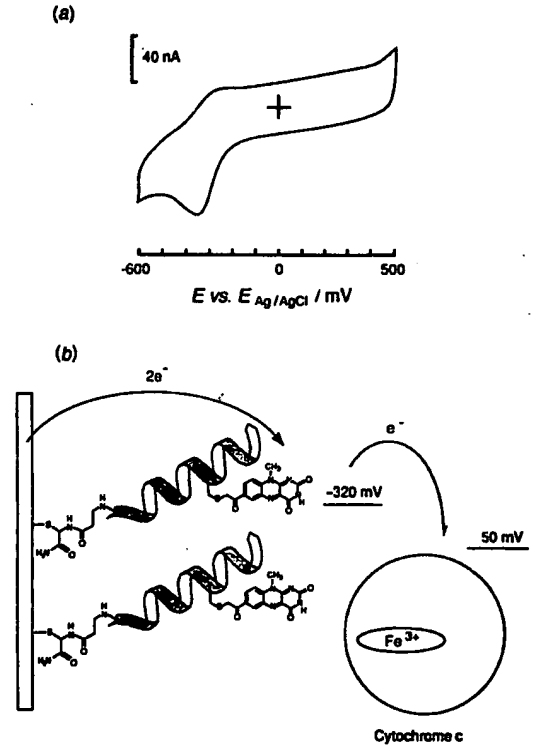

Fig. 7 (*a*) Cyclic voltammogram for the gold electrode modified with the Fla^8-1α-SH in 5.0×10^{-5} mol dm^{-3} cyctochrome c–0.1 mol dm^{-3} phosphate buffer, pH 7.0 at 25 °C; the sweep rate was 10 mV s^{-1}. (*b*) Illustration of the electron transfer from the electrode to cyctochrome c mediated by Fla-1α-SH bound on the gold surface.

Fig. 7 shows the cyclic voltammogram of the Fla^8-1α-SH-modified electrode in the presence of cytochrome c in the buffer. In a similar manner to the $Fe(CN)_6^{3-}$ ion, the cyclic voltammogram showed an enhancement in the peak at the reduction potential (−325 mV) of Fla^8-1α-SH. This result indicated the catalytic reduction of cytochrome c by the flavin on the peptide. Although the detailed mechanism on the interaction or electron transfer between cytochrome c and Fla-1α-SH bound on the electrode remains unknown, the Fla-peptide on the electrode could mediate the electron transfer from the electrode to the haem protein in a vector manner.

Conclusions

It has been demonstrated that flavin-conjugated α-helix peptides are adsorbed on a gold electrode surface through the sulfide linkage. This is the first example of the adsorption of peptides conjugated with functionalized chromophores on a gold surface. The cyclic voltammetry revealed that the functional group, flavin, was redox-active on the electrode. By the use of flavin as an electrochemical probe, we could obtain information about the peptide assembly and properties on the gold surface. Additionally, the flavin-conjugated peptides could mediate the electron transfer from the electrode to $Fe(CN)_6^{3-}$ ion or cytochrome c in a vector manner. Though the detailed study on the orientation and the conformation of peptides on an electrode surface could be carried out to elucidate the relationship between the oriented functional group in the polypeptide 3D structure and electronic functions, the information obtained by future efforts will realize the application of the *de novo* designed functional polypeptides to new intelligent materials, such as electronic devices and chemical sensors.

Experimental

Materials and methods

All chemicals and solvents were of reagent or HPLC grade. Amino acid derivatives and reagents for peptide synthesis were purchased from Watanabe Chemical Co. (Hiroshima, Japan). Solid-phase peptide synthesis was carried out manually in a polypropylene column. Matrix assisted laser desorption time-of-flight mass spectra (TOFMS) were measured on a Shimadzu MALDI III mass spectrometer by using 3,5-dimethoxy-4-hydroxycinnamic acid as a matrix. Fast atom bombardment mass spectra (FABMS) were recorded on a JEOL JMS-DX-300 mass spectrometer equipped with JEOL JMA-3100 mass data analysis system by using *threo*-1,4-dimercaptobutane-2,3-diol (DTT) as a matrix and xenon for bombardment. Amino acid analyses were carried out on a JEOL JLC-300 system with ninhydrin detection after hydrolysis in 6.0 mol dm^{-3} HCl at 110 °C for 24 h in a sealed tube. HPLC was carried out on a Wakosil 5C18 column (Wako Pure Chemical Industries) (4.6 × 150 mm) or a YMC ODS A-323 column (YMC Co.) (10 × 250 mm) by employing a Hitachi L-7100 intelligent pump equipped with a Hitachi L-7400 UV–VIS detector and a Hitachi D-7500 chromato-integrator. Solvent systems for HPLC are shown in the text. FT-IR spectra were recorded on a Perkin-Elmer 1600 series FT-IR spectrometer using Fla-1α-SH cast film formed from TFE solution on a calcium fluoride plate.

7α-Bromoacetyl-10-methylisoalloxazine. 7-Acetyl-10-methylisoalloxazine[18a] was a gift from Professor Norikazu Nishino, Kyushu Institute of Technology. 7α-Bromoacetyl-10-methylisoalloxazine was synthesized according to the method of Levine and Kaiser with some modifications.[18a] 7-Acetyl-10-methylisoalloxazine (Fla) (135 mg, 0.5×10^{-3} mol) was dissolved in acetic acid (15 cm^3) at 85–90 °C. Bromine in acetic acid (0.25 mol dm^{-3}, 2.0 cm^3, 1.0 equiv.) was added dropwise to the solution over 20 min. The solution was then stirred for an additional 10 min at 85–90 °C and cooled to room temperature resulting in the precipitation of the product. The crystals were filtered and washed with diethyl ether. The crystals contained a small amount (<5% on HPLC) of starting material and dibrominated flavin in the acetyl group. Because the presence of a small amount of the by-products did not have a significant effect on the modification of the peptide by 7α-bromoacetyl-10-methylisoalloxazine, the modifying reagent was used without further purification.

Peptide synthesis

Cys^6-, Cys^7- and Cys^8-1α. Fmoc-Ala-Leu-Glu(OBu^t)-Gln-(Trt)-Lys(OBu^t)-Cys(Trt)-Ala-Ala-Leu-Glu(OBu^t)-Gln(Trt)-

Lys(Boc)-Leu-Ala-βAla-Cys(Acm)-NH-SAL resin, Fmoc-Ala-Leu-Glu(OBu')-Gln(Trt)-Lys(Boc)-Leu-Cys(Trt)-Ala-Leu-Glu(OBu')-Gln(Trt)-Lys(Boc)-Leu-Ala-βAla-Cys(Acm)-NH-SAL resin and Fmoc-Ala-Leu-Glu(OBu')-Gln(Trt)-Lys(Boc)-Leu-Ala-Cys(Trt)-Leu-Glu(OBu')-Gln(Trt)-Lys(Boc)-Leu-Ala-βAla-Cys(Acm)-NH-SAL resin (Bu', *tert*-butyl; Trt, trityl; Boc, *tert*-butyloxycarbonyl; Acm, acetamidomethyl) were synthesized manually by stepwise elongation of Fmoc-amino acids on 4-(2',4'-dimethoxyphenylaminomethyl)phenoxy resin (NH-SAL resin).[27] The following procedure was repeated from Fmoc-NH-SAL resin (0.50 g, 0.24 mmol amine); (i) washing with 1-methyl-2-pyrrolidone (NMP) (×5), (ii) washing with 20% piperidine (PPD)–NMP (×1), (iii) deprotection with 20% PPD–NMP (15 min), (iv) washing with NMP (×10), (v) coupling with Fmoc-AA [Fmoc-Ala·H_2O, Fmoc-β-Ala, Fmoc-Cys(Acm), Fmoc-Cys(Trt)·0.5EtOAc, Fmoc-Gln(Trt), Fmoc-Glu(OBu')·H_2O, Fmoc-Leu, Fmoc-Lys(Boc)] (4.0 equiv.), benzotriazol-1-yloxytris(dimethylamino)phosphonium hexafluorophosphate (BOP) (4.0 equiv.), 1-hydroxybenzotriazole hydrate (HOBt·H_2O) (4.0 equiv.) and dipropan-2-ylethylamine (DIEA) (8.0 equiv.) in NMP (15 min), (vi) washing with NMP (×5). Solvent volumes were 2.0 cm^3. Coupling efficiency was checked by the Kaiser test.[34] To synthesize Ac-peptide resin, the Fmoc-deprotected peptide resin was treated with acetic anhydride (10 equiv.) and DIEA (5.0 equiv.) in dichloromethane for 20 min.

To remove the resin and protecting groups except for the Acm group, the peptide resin was stirred in TFA (9.6 cm^3) in the presence of *m*-cresol (0.24 cm^3), ethane-1,2-dithiol (0.72 cm^3) and thioanisole (1.44 cm^3) as scavengers for 1 h at 25 °C. The resin was filtered and washed five times with TFA. The solvent was evaporated and the residues were solidified with diethyl ether in an ice-bath to give crude peptides: Cys^6-1α [420 mg (99%)], Cys^7-1α- [360 mg (84%)] and Cys^8-1α [360 mg (82%)].

All crude peptides were purified by HPLC on a YMC ODS A-323 column (10 × 250 mm) using a linear gradient of 30–50% acetonitrile–0.1% TFA (30 min) to give the product with a single peak on analytical HPLC (Wakosil 5C18, 4.6 × 150 mm with a linear gradient of 20–60% acetonitrile–0.1% TFA over 30 min): Cys^6-1α (48%), Cys^7-1α (35%) and Cys^8-1α (37%). Peptides were identified by the molecular ion peak $(M + H)^+$, $(M + Na)^+$ and $(M + K)^+$ on FAB-MS; Ac-Ala-Leu-Glu-Gln-Lys-Cys-Ala-Ala-Leu-Glu-Gln-Lys-Leu-Ala-βAla-Cys(Acm)-NH_2, *m/z* 1801 $[(M + H)^+]$, 1823 $[(M + Na)^+]$ and 1839 $[(M + K)^+]$; Ac-Ala-Leu-Glu-Gln-Lys-Leu-Cys-Ala-Leu-Glu-Gln-Lys-Leu-Ala-βAla-Cys(Acm)-NH_2, *m/z* 1844 $[(M + H)^+]$; Ac-Ala-Leu-Glu-Gln-Lys-Leu-Ala-Cys-Leu-Glu-Gln-Lys-Leu-Ala-βAla-Cys(Acm)-NH_2, *m/z* 1844 $[(M + H)^+]$.

Fla^6-, Fla^7- and Fla^8-1α. To a solution of 7α-bromoacetyl-10-methylisoalloxazine (17 mg, 5.0×10^{-5} mol) in TFE (5.0 cm^3), Cys-1α peptide (45 mg, 2.5×10^{-5} mol) in 0.1 mol dm^{-3} Tris·HCl buffer, pH 7.5 (5.0 cm^3) was added in one portion. The solution was stirred at room temperature for 3–4 h, keeping the pH of the solution at 7.5. The solvent was evaporated and the residues were dissolved in 10% acetic acid (1.0 cm^3). Subsequently, the peptide solution was subjected to a Sephadex G-25 gel permeation column (2.2 × 45 cm) pre-equilibrated with 10% acetic acid. The column was eluted with 10% acetic acid and the desired fractions were collected. The peptide conjugated with flavin was detected by the absorption at 350 nm. After evaporation, the residue was dissolved in water. The aqueous solution was lyophilized to give the product with a single peak on analytical HPLC (Wakosil 5C18, 4.6 × 150 mm with a linear gradient of 20–60% acetonitrile–0.1% TFA over 30 min): Fla^6-1α [37 mg (70%)], Fla^7-1α [36 mg (68%)] and Fla^8-1α [38 mg (72%)]; TOFMS; Ac-Ala-Leu-Glu-Gln-Lys-Cys(Fla)-Ala-Ala-Leu-Glu-Gln-Lys-Leu-Ala-βAla-Cys(Acm)-NH_2 (Fla^6-1α), *m/z* 2072.4 $[(M + H)^+]$ (calc. 2071.4); Ac-Ala-Leu-Glu-Gln-Lys-Leu-Cys(Fla)-Ala-Leu-Glu-Gln-Lys-Leu-Ala-βAla-Cys(Acm)-NH_2 (Fla^7-1α), *m/z* 2114.1 $[(M + H)^+]$ (calc. 2113.5); Ac-Ala-Leu-Glu-Gln-Lys-Leu-Ala-Cys(Fla)-Leu-Glu-Gln-Lys-Leu-Ala-βAla-Cys(Acm)-NH_2 (Fla^8-1α), *m/z* 2113.8 $[(M + H)^+]$ (calc. 2113.5); Fla^6-1α (2.0×10^{-5} mol dm^{-3}), λ_{max}(2.0×10^{-2} mol dm^{-3} Tris·HCl buffer, pH 7.4)/nm 430 (ε/dm^3 mol^{-1} cm^{-1} 10 900), 349 (5010) and 289 (30 100); λ_{max}(TFE)/nm 430 (11 200), 349 (5060) and 288 (35 100); Fla^7-1α (2.0×10^{-5} mol dm^{-3}), λ_{max}(Tris·HCl buffer, pH 7.4)/nm 430 (10 900), 349 (5200) and 289 (30 700); λ_{max}(TFE)/nm 430 (11 200), 349 (5200) and 288 (34 500); Fla^8-1α (2.0×10^{-5} mol dm^{-3}), λ_{max}(Tris·HCl buffer, pH 7.4)/nm 430 (10 900), 349 (5190) and 289 (31 500); λ_{max}(TFE)/nm 430 (11 200), 349 (5830) and 288 (34 400); amino acid analysis; Fla^6-1α: $Ala_{4.00}$ (4), $Glu_{3.94}$ (4), $Leu_{3.02}$ (3), $Lys_{1.96}$ (2); Fla^7-1α: $Ala_{3.00}$ (3), $Glu_{4.10}$ (4), $Leu_{3.98}$ (4), $Lys_{1.95}$ (2); Fla^8-1α: $Ala_{3.00}$ (3), $Glu_{3.94}$ (4), $Leu_{3.99}$ (4), $Lys_{2.02}$ (2).

Fla^6-, Fla^7- and Fla^8-1α-SH. To remove the Acm group of Cys^{16} in each peptide, Fla-1α-peptide (21 mg, 1.0×10^{-5} mol) was dissolved in TFA (2.0 cm^3) and the solution was stirred with $AgBF_4$ (20 equiv.) in the presence of anisole (10 equiv.) at 0 °C for 1 h. The peptide–Ag salt, precipitated with diethyl ether, was stirred with DTT (40 equiv.) in 10% acetic acid at room temperature for 3 h. After centrifugation, the supernatant was subjected to a Sephadex G-25 gel permeation column (2.2 × 45 cm) preequilibrated with 10% acetic acid. The column was eluted with 10% acetic acid and the desired fractions were collected. After evaporation, the residues were dissolved in water. The aqueous solution was lyophilized to give the product with a single peak on analytical HPLC (Wakosil 5C18, 4.6 × 150 mm with a linear gradient of 20–60% acetonitrile–0.1% TFA over 30 min): Fla^6-1α-SH [12 mg (60%)], Fla^7-1α-SH [13 mg (64%)], Fla^8-1α-SH [16 mg (78%)]; TOFMS; Ac-Ala-Leu-Glu-Gln-Lys-Cys(Fla)-Ala-Ala-Leu-Glu-Gln-Lys-Leu-Ala-βAla-Cys-NH_2, *m/z* 2000.6 $[(M + H)]$ (calc. 2000.3); Ac-Ala-Leu-Glu-Gln-Lys-Leu-Cys(Fla)-Ala-Leu-Glu-Gln-Lys-Leu-Ala-βAla-Cys-NH_2, *m/z* 2042.3 $[(M + H)^+]$ (calc. 2042.4); Ac-Ala-Leu-Glu-Gln-Lys-Leu-Ala-Cys-(Fla)-Leu-Glu-Gln-Lys-Leu-Ala-βAla-Cys-NH_2, *m/z* 2044.4 $[(M + H)^+]$ (calc. 2042.4); FT-IR (cast film from TFE solution); Fla^6-1α-SH, amide I 1656 cm^{-1}, amide II 1547 cm^{-1}; Fla^7-1α-SH, amide I 1651 cm^{-1}, amide II 1541 cm^{-1}; Fla^8-1α-SH, amide I 1654 cm^{-1}, amide II 1544 cm^{-1}.

Fla^6-, Fla^7- and Fla^8-2α. To form a disulfide bond by air oxidation, Fla-1α-SH (12 mg, 6.0×10^{-6} mol) was dissolved in TFE (0.5 cm^3) and to the solution was added 0.1 mol dm^{-3} Tris·HCl buffer, pH 8.0 (0.5 cm^3). The peptide solution was vigorously stirred at room temperature for 24 h. The reaction was stopped by the addition of 10% acetic acid (1.0 cm^3) and the peptide was purified by gel filtration with Sephadex G-25 (2.2 × 45 cm, 10% acetic acid). The desired fractions were collected and the solvent was evaporated. The residues were dissolved in water and the aqueous solution was lyophilized to give the 2α-peptides: Fla^6-2α [6.4 mg (54%)], Fla^7-2α [7.8 mg (63%)], Fla^8-2α [7.8 mg (63%)]; TOFMS; Fla^6-2α, *m/z* 4001.4 $[(M + H)^+]$ (calc. 3997.6); Fla^7-2α, *m/z* 4086.8 $[(M + H)^+]$ (calc. 4081.8); Fla^8-2α, *m/z* 4086.6 $[(M + H)^+]$ (calc. 4081.8); Fla^6-2α (1.0×10^{-5} mol dm^{-3}), λ_{max}(2.0×10^{-2} mol dm^{-3} Tris·HCl buffer, pH 7.4)/nm 430 (ε/dm^3 mol^{-1} cm^{-1} 21 000), 349 (12 280) and 286 (62 000); λ_{max}(TFE)/nm 431 (22 400), 349 (12 180) and 286 (69 000); Fla^7-2α (1.0×10^{-5} mol dm^{-3}), λ_{max}(Tris·HCl buffer, pH 7.4)/ nm 430 (21 200), 349 (10 780) and 288 (62 200); λ_{max}(TFE)/ nm 432 (22 400), 349 (11 340) and 287 (69 800); Fla^8-2α (1.0×10^{-5} mol dm^{-3}), λ_{max}(Tris·HCl buffer, pH 7.4)/nm 430 (19 080), 349 (12 500) and 287 (58 200); λ_{max}(TFE)/nm 432 (22 000), 349 (14 060) and 285 (69 000); amino acid analysis; Fla^6-2α: $Ala_{8.00}$ (8), $Glu_{7.84}$ (8), $Leu_{6.06}$ (6), $Lys_{3.76}$ (4); Fla^7-2α: $Ala_{6.00}$ (6), $Glu_{7.90}$ (8), $Leu_{7.96}$ (8), $Lys_{3.88}$ (4); Fla^8-2α: $Ala_{6.00}$ (6), $Glu_{7.92}$ (8), $Leu_{8.00}$ (8), $Lys_{3.92}$ (4).

Fluorescence measurements

Fluorescence spectra were measured on a Hitachi F-3010

fluorescence spectrophotometer. Peptides were dissolved in 2.0×10^{-3} mol dm^{-3} Tris·HCl buffer (pH 7.4) or TFE in Fla-1α and Fla-2α concentrations of 2.0×10^{-5} and 1.0×10^{-5} mol dm^{-3}, respectively.

CD measurements

CD spectra were recorded on a Jasco J-720 spectropolarimeter using a quartz cell with 1.0 of 10 mm pathlength. Peptides were dissolved in 2.0×10^{-2} mol dm^{-3} Tris·HCl buffer (pH 7.4) or TFE in Fla-1α and Fla-2α concentrations of 2.0×10^{-5} and 1.0×10^{-5} mol dm^{-3}, respectively.

CV measurements

Fla-1α-SH modified electrodes were prepared by the following procedure. A gold disk working electrode (Bioanalytical System, surface area 2.01×10^{-2} cm^2) was polished with diamond paste (particle size 10×10^{-5} m) and sonicated in water for 10 min using a bath type sonicator (Yamato Branson 3200). Again, the gold electrode was polished with alumina powder (particle size 4.0×10^{-8} m) and rinsed with water and then acetone. Subsequently, the electrode was immersed in Fla-1α-SH (1.0×10^{-3} mol dm^{-3}) in water for 10 h, and then sonicated in TFE and water for 10 min, respectively, to remove the non-specifically bound peptides. Cyclic voltammograms were measured in deoxygenated 0.1 mol dm^{-3} phosphate buffer, pH 7.0, as a supporting electrolyte. A home-made single-compartment glass cell was used for the experiment. A gold electrode was used as the counter-electrode. Ag/AgCl (SCE − 49 mV) was used as the reference electrode. The experiments were carried out in Huso Electro Chemical System 315B Cyclic Voltammograph equipped with Graphtec WX1000. Bovine heart cytochrome c for cyclic voltammetry measurements was purchased from Sigma and purified with an ion exchange CM-25 column.

Acknowledgements

We are grateful to Dr N. Nishino, Kyushu Institute of Technology, for the generous gift of 7-acetyl-10-methylisoalloxazine and to Dr T. Sagara, Nagasaki University, for helpful suggestions. This work was funded in part by a Grant-in-Aid for Scientific Research from the Ministry of Education, Science, Culture and Sports, Japan.

References

1 S. F. Betz, D. P. Raleigh and W. F. DeGrado, *Curr. Opin. Struct. Biol.*, 1993, **3**, 601; W. F. DeGrado, Z. R. Wasserman and J. D. Lear, *Science*, 1989, **243**, 622; L. Regan and W. F. DeGrado, *Science*, 1988, **241**, 976.
2 M. Mutter and S. Vuilleumier, *Angew. Chem., Int. Ed. Engl.*, 1989, **28**, 535; M. Mutter, G. G. Tuchscherer, C. Miller, K.-H. Altmann, R. I. Carey, D. F. Wyss, A. M. Labhardt and J. E. Rivier, *J. Am. Chem. Soc.*, 1992, **114**, 1463.
3 K. W. Hahn, W. A. Klis and J. M. Stewart, *Science*, 1990, **248**, 1544.
4 M. Montal, M. S. Montal and J. M. Tomich, *Proc. Natl. Acad. Sci. USA*, 1990, **87**, 6929.
5 H. Morii, K. Ichimura and H. Uedaira, *Chem. Lett.*, 1990, 1987; *Proteins Str. Func. Genet.*, 1991, **11**, 133; H. Morii, S. Honda, K. Ichimura and H. Uedaira, *Bull. Chem. Soc. Jpn.*, 1991, **64**, 396.
6 T. Sasaki and E. T. Kaiser, *J. Am. Chem. Soc.*, 1989, **111**, 380; T. Sasaki and E. T. Kaiser, *Biopolymers*, 1990, **29**, 79; M. Leiberman and T. Sasaki, *J. Am. Chem. Soc.*, 1991, **113**, 1470; T. Sasaki and M. Lieberman, *Tetrahedron*, 1993, **49**, 3677.
7 M. R. Ghadiri, C. Soares and C. Choi, *J. Am. Chem. Soc.*, 1992, **114**, 825; 4000.
8 C. T. Choma, J. D. Lear, M. J. Nelson, P. L. Dutton, D. E. Robertson and W. F. DeGrado, *J. Am. Chem. Soc.*, 1994, **116**, 856; D. E. Robertson, R. S. Farid, C. C. Mosser, J. L. Urbauer, S. E. Mulholland, R. Pidikiti, J. D. Lear, A. J. Wand,. W. F. DeGrado and P. L. Dutton, *Nature*, 1994, **368**, 425; F. Rabanal, W. F. DeGrado and P. L. Dutton, *J. Am. Chem. Soc.*, 1996, **118**, 473.
9 (*a*) H. Mihara, Y. Tanaka, T. Fujimoto and N. Nishino, *J. Chem. Soc., Perkin Trans. 2*, 1995, 1133; (*b*) H. Mihara, Y. Tanaka, T. Fujimoto and N. Nishino, *J. Chem. Soc., Perkin Trans. 2*, 1995, 1915; (*c*) H. Mihara, N. Nishino and T. Fujimoto, *Chem. Lett.*, 1992, 1809; (*d*) S. Ono, N. Kameda, T. Yoshimura, C. Shimasaki, E. Tsukurimichi, H. Mihara and N. Nishino, *Chem. Lett.*, 1995, 965; (*e*) N. Nishino, H. Mihara, Y. Tanaka and T. Fujimoto, *Tetrahedron Lett.*, 1992, **33**, 5767.
10 (*a*) H. Mihara, N. Nishino, R. Hasegawa, T. Fujimoto, S. Usui, H. Ishida and K. Ohkubo, *Chem. Lett.*, 1992, 1813; (*b*) H. Mihara, Y. Haruta, S. Sakamoto, N. Nishino and H. Aoyagi, *Chem. Lett.*, 1996, 1; (*c*) H. Mihara, K. Tomizaki, T. Fujimoto, S. Sakamoto, H. Aoyagi and N. Nishino, *Chem. Lett.*, 1996, 187; (*d*) H. Mihara, K. Tomizaki, N. Nishino and T. Fujimoto, *Chem. Lett.*, 1993, 1533.
11 D. R. Benson, B. R. Hart, X. Zhu and M. B. Doughty, *J. Am. Chem. Soc.*, 1995, **117**, 8502.
12 E. U. Thoden van Velzen, J. F. J. Engbersen and D. N. Reinhoudt, *J. Am. Chem. Soc.*, 1994, **116**, 3597; K. D. Schierbaum, T. Weiss, E. U. Thoden van Velzen, J. F. J. Engbersen, D. N. Reinhoudt and W. Göpel, *Science*, 1994, **265**, 1413; E. U. Thoden van Velzen, J. F. J. Engbersen, P. J. de Lange, J. W. G. Mahy and D. N. Reinhoudt, *J. Am. Chem. Soc.*, 1995, **117**, 6853.
13 M. T. Rojas, R. Königer, J. F. Stoddart and A. E. Kaifer, *J. Am. Chem. Soc.*, 1995, **117**, 336.
14 M. Maeda, K. Nakano, S. Uchida and M. Takagi, *Chem. Lett.*, 1994, 1805.
15 T. Akiyama, H. Imahori and Y. Sakata, *Chem. Lett*, 1994, 1447.
16 M. Lion-Dagan, E. Katz and I. Willner, *J. Am. Chem. Soc.*, 1994, **116**, 7913.
17 (*a*) J. K. Whitesell and H. K. Chang, *Science*, 1993, **261**, 73; (*b*) D. J. van den Heuvel, R. P. H. Kooyman, J. W. Drijfhout and G. W. Welling, *Anal. Biochem.*, 1993, **215**, 223.
18 (*a*) H. L. Levine and E. T. Kaiser, *J. Am. Chem. Soc.*, 1978, **100**, 7670; (*b*) S. E. Rokita and E. T. Kaiser, *J. Am. Chem. Soc.*, 1986, **108**, 4984; (*c*) D. Hilvert and E. T. Kaiser, *J. Am. Chem. Soc.*, 1985, **107**, 5805.
19 H. Durliat and M. Comtat, *J. Biol. Chem.*, 1987, **262**, 11497.
20 V. I. Birss, H. Elzanowska and R. A. Turner, *Can. J. Chem.*, 1988, **66**, 86.
21 L. Gorton and G. Johansson, *J. Electroanal. Chem.*, 1980, **113**, 151.
22 C. N. Durfor, B. A. Yenser and M. L. Bowers, *J. Electroanal. Chem.*, 1988, **244**, 287.
23 S. Berchmans and R. Vijayavalli, *Langmuir*, 1995, **11**, 286.
24 S. Ueyama, S. Isoda and M. Maeda, *J. Electroanal. Chem.*, 1989, **264**, 149; S. Ueyama, S. Isoda and M. Maeda, *J. Electroanal. Chem.*, 1990, **293**, 125.
25 (*a*) N. E. Zhou, B.-Y. Zhu, C. M. Kay and R. S. Hodges, *Biopolymers*, 1992, **32**, 419; (*b*) J. Talbot and R. S. Hodges, *Acc. Chem. Res.*, 1982, **15**, 224; (*c*) E. K. O'Shea, J. D. Klemm, P. S. Kim and T. Alber, *Science*, 1991, **254**, 539.
26 E. Atherton and R. C. Sheppard, *Solid Phase Peptide Synthesis: A Practical Approach*, IRL Press, Oxford, England, 1989.
27 H. Rink, *Tetradrondron Lett*, 1987, **28**, 3787.
28 M. Yoshida, T. Tatsumi, Y. Fujiwara, S. Iinuma, T. Kimura, K. Akaji and Y. Kiso, *Chem. Pharm. Bull.*, 1990, **38**, 1551.
29 M. C. Falk and D. B. McCormick, *Biochemistry*, 1976, **15**, 646.
30 J. M. Scholtz, H. Qian, E. J. York, J. M. Stewart and R. L. Baldwin, *Biopolymers*, 1991, **31**, 1463.
31 V. Massey and G. Palmer, *Biochemistry*, 1995, **5**, 3181.
32 A. Mattevi, G. Obmolova, K. Kalk, W. van Berkel and W. Hol, *J. Mol. Biol.*, 1993, **230**, 1200.
33 J. F. Rabolt, W. H. Moore and S. Krimm, *Macromolecules*, 1977, **10**, 1065.
34 K. Kaiser, R. L. Colescott and C. T. Bossinger, *Anal. Biochem.*, 1970, **34**, 595.

Paper 6/03199D
Received 7th *May* 1996
Accepted 26th *June* 1996

Borrower's Name	Alex Noguerola	Org. or A.U.	1744	Phone	305-568-6
Serial Number	09/044,350	Date of Request	6/16/99	Date Needed By	9/16/99

Please Attach Copy of Abstract, Citation, Or Bibliography. If Available Please Provide Complete Citation. Only One Request Per Form.

Author/Editor:	See attached sheet.
Journal/Book Title:	
Article Title:	
Volume (Issue):	
Pages:	
Year of Publication:	
Publisher:	
Remarks:	

STIC Use Only TP248.13.C87 Accession Number: 2533938

LIBRARY ACTION	LC		NAL		NIH		NLM		NBS		PTO		OTHER	
	1st	2nd	1st	2nd	1st	2nd	1st	2nd	1st	2nd	1st	2nd	1st	2nd
Local Attempts														
Date														
Initials														
Results														
Examnr. Called														
Page Count														
Money Spent														

Provided By: Source and Date

Ordered From: Source and Date

Remarks/Comments
- 1st & 2nd denotes times taken to a library
- FX - Means Faxed to us
- O/N - Under NLM=Overnight Service

COMPLETED

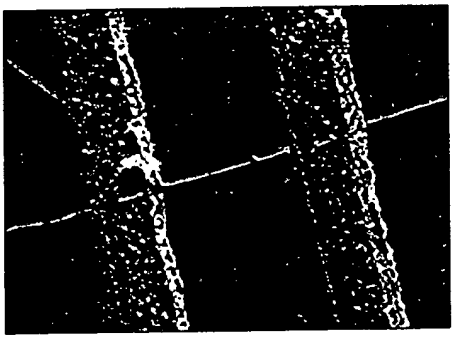

Atomic force microscope image of a single carbon nanotube crossing two platinum strips, which are used as source and drain contacts. On the right, a part is seen of a third electrode which could be used as a gate. The distance between electrodes is 200 nm. In the upper left corner a short tube is seen. [Courtesy of S. J. Tans *et al.*, Delft University of Technology]

and also supplied the nanotubes used in the two recent transport experiments. Tans and colleagues (*4*), from Delft, have studied a single nanotube, and Bockrath and colleagues (*5*), from Berkeley, measured a bundle of nanotubes (see page 1922). The two groups found similar electron transport properties.

So, what is special about these transistor characteristics? As we know, electrons in molecules only occupy quantized orbitals, which correspond to discrete levels in the energy spectrum. The current from source to drain contacts is carried exclusively by electrons that have exactly these particular energies. If one adds an electron to the molecule, one needs to pay more than just the finite energy to occupy the next available molecular state; one must also pay a so-called charging energy to compensate for the extra elementary charge that the molecule now contains. Therefore, both quantization of charge and quantized molecular states govern the electronic properties of a molecular transistor. The energy required to add an electron to the molecule can either be supplied by the voltage source between the two current contacts or by the voltage applied to the gate terminal. These voltages are the spectroscopic tools in the determination of the charging energies and the molecular states (*2–5*).

The physics of charging energies and discrete energy states has been exploited before by the mesoscopic community. These quantum effects were found in ultrasmall transistors known as quantum dots. Those quantum dot transistors are small electron boxes with zero dimensionality fabricated in semiconductor materials. Because charging energy and quantized states resemble so closely the ionization energy and excitation energies of an atom, quantum dots are often nicknamed "artificial atoms" (*8*). Following the same arguments, two or more coupled quantum dots can be regarded as "artificial molecules" (*9*). We can complete the connection between natural and artificial structures by naming the single-molecule transistor a "natural quantum dot." The finite length of the nanotubes makes them effectively zero-dimensional, that is, the same as quantum dots. And indeed, the present transport experiments on carbon nanotubes are well explained by the theory developed for quantum dots (*4*, *5*). The hope is that in future experiments, the physical consequences from the narrow and long geometry will be revealed. One-dimensional conductors have attracted a lot of theoretical interest because they are model systems for strongly interacting many-body physics. Maybe the carbon nanotubes will serve as the experimental system in which these exotic theories can be tested.

Whereas quantum dots show their quantum properties only when cooled to low temperatures (a few kelvin above absolute zero), the small size of single-molecule transistors allow them to operate at much higher temperatures. In fact, scanning tunneling studies on a C_{60} molecule by Porath and Millo (*2*) and on a carbon cluster by Soldatov *et al.* (*3*) still show transistor operation at room temperature. In this transistor, a single electron again makes the difference between an on state and an off state. Although the persistence up to room temperature is very promising, we still have a long way to go before we can integrate or couple different nanotubes to make a little electronic circuits. On the other hand, nanotubes have an interesting connection between their mechanical and electrical properties. For instance, a kink in a nanotube can change it from metallic to semiconducting (*10*). So, one can imagine building a specific electronic circuit by stretching and bending a couple of nanotubes here and there.

References

1. R. Feynman, *Science* **254**, 1300 (1991).
2. D. Porath and O. Millo, *J. Appl. Phys.* **81**, 2241 (1996).
3. E. S. Soldatov *et al.*, in preparation; also available from the Los-Alamos e-Print archive at: http://xxx.lanl.gov/abs/cond-mat/9610155
4. S. J. Tans *et al.*, *Nature*, in press.
5. M. Bockrath *et al.*, *ibid.* **275**, 1922 (1997).
6. R. F. Service, *ibid.* **274**, 345 (1996).
7. A. Thess *et al.*, *Science* **273**, 483 (1996).
8. M. Kastner, *Phys. Today* **46**, 24 (January 1993); R. C. Ashoori, *Nature* **379**, 413 (1996).
9. L. Kouwenhoven, *Science* **268**, 1440 (1995).
10. M. Dresselhaus, *Phys. World* **9**,18 (May 1996).

IMMUNOLOGY

A Gut Reaction: Lymphoepithelial Communication in the Intestine

Fergus Shanahan

Different parts of the body require different defenses against pathogens. The immune system is therefore regionally specialized and compartmentalized, in large part by the conditioning effect of the local microenvironment. On page 1937 of this issue, Wang and colleagues focus on the intestine and provide important new insight into the immunoregulatory effects on intestinal T cells of local hormonal networks, specifically thyrotropin-releasing hormone (TRH) and thyroid-stimulating hormone (TSH) (*1*). Their work illustrates the importance of studying the immune system in its natural environment.

The intestinal mucosa separates the external environment (the gut) from the internal milieu, forming the most extensive of such barriers in the body. The large surface area facilitates effective absorption of essential nutrients, but presents a problem—only a single layer of epithelium separates the intestinal lumen from the internal environment. So this anatomic design may not be optimal for excluding infectious, toxic, and otherwise harmless immunogenic material from the body. The dilemma is solved by adaptation of versatile immunologic and nonimmunologic defenses (*2*).

Strategic adaptation of the intestinal immune system is reflected in the molecular and cellular components of the mucosal immune system, which differ in several respects from their counterparts at other sites within the systemic immune system (*2*). Interspersed among the epithelial cells (enterocytes) lining the intestine are the intraepithelial lymphocytes (IELs) (see figure). The IELs are an important immunologic compartment; collectively, they represent a pool of cells comparable in size to that of all peripheral lymphocytes in the spleen. They are not only functionally and phenotypically distinct

The author is in the Department of Medicine, National University of Ireland, Cork University Hospital, Cork, Ireland. E-mail: fshanahan@iruccvax.ucc.ie

Borrower's Name	Alex Noguerola	Org. or A.U.	1744	Phone	305-5686
Serial Number	09/044,350	Date of Request	6/16/99	Date Needed By	9/16/99

Please Attach Copy of Abstract, Citation, Or Bibliography. If Available Please Provide Complete Citation. Only One Request Per Form.

Author/Editor:	See attached sheet
Journal/Book Title:	
Article Title:	
Volume (Issue):	
Pages:	
Year of Publication:	
Publisher:	
Remarks:	

STIC Use Only DLC

Accession Number: 253936

LIBRARY ACTION	LC		NAL		NIH		NLM		NBS		PTO		OTHER	
	1st	2nd	1st	2nd	1st	2nd	1st	2nd	1st	2nd	1st	2nd	1st	2nd
Local Attempts														
Date														
Initials														
Results														
Examnr. Called														
Page Count														
Money Spent														

Provided By: Source and Date

Ordered From: Source and Date

LHL 6-16

Remarks/Comments
- 1st & 2nd denotes times taken to a library
- FX - Means Faxed to us
- O/N - Under NLM=Overnight Service

of the circle shown in Fig. 3A. However, because the tip would have to be moved from one cluster position to the next, controlled by the microprocessor, this method would be much slower (approximately by a factor of 10) than cluster production during scanning. Although 400 Cu clusters were produced during a very short time, there was no indication of Cu depletion at the tip as all clusters are nearly identical in size (height h = 0.6 nm, FWHM = 3.5 nm). This result suggests that the Cu reservoir at the tip is continuously refilled as a result of permanent Cu deposition from solution (tip potential $E_{tip} = -30$ mV versus Cu/Cu^{2+}).

Continuous structures can also be generated with microprocessor-controlled cluster formation by placing the Cu clusters very close together so that they can contact each other. For example, we have produced nanometer-sized "conducting wires" with a FWHM of 3 to 4 nm and a length of several hundred nanometers on Au(111) (*19*).

In addition to precisely positioning individual Cu clusters with identical heights, it is also possible with this system to vary the size of the deposited clusters in a controlled manner within certain limits. This can be done by varying the extent of the tip approach with the external z pulse, which controls the amount of Cu transferred from the tip to the Au surface (Fig. 5, A and B). In general, the cluster height increases with increasing z-pulse height, but, above a tip displacement of $\Delta z \approx 1.2$ nm, the cluster height did not increase further and holes appeared in the surface instead. This result suggests that the tip displacement became too large and the tip struck the substrate.

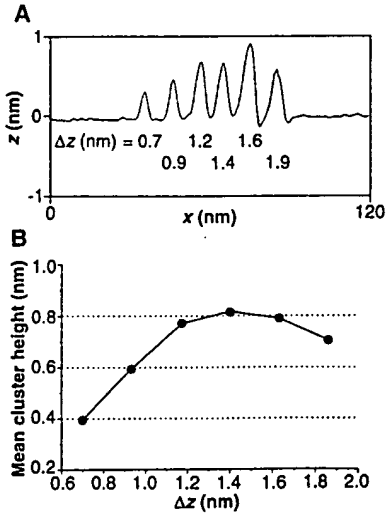

Fig. 5. (**A**) Cross section of six Cu clusters in a row on Au(111) in 0.05 M H_2SO_4 + 1 mM $CuSO_4$, which demonstrates the variation of cluster height with the z-pulse height. The corresponding tip displacement Δz is shown in the figure. Pulse duration of Δt = 10 ms; E_{sample} = +10 mV; E_{tip} = −50 mV; I_T = 2 nA. (**B**) Mean cluster height, as derived from 15 experiments, as a function of the tip displacement Δz used to generate the Cu clusters. The dotted lines indicate the height of a Cu monolayer. E_{sample} = +10 mV; E_{tip} = −50 mV; I_T = 2 nA.

REFERENCES AND NOTES

1. G. Binnig, H. Rohrer, Ch. Gerber, E. Weibel, *Phys. Rev. Lett.* **49**, 57 (1982).
2. See, for example, C. F. Quate, *Highlights in Condensed Matter Physics and Future Prospects*, L. Esaki, Ed. (NATO Advanced Study Institutes, Plenum, New York, 1991), vol. B285, p. 573.
3. R. S. Becker, J. A. Golovchenko, B. S. Swartzentruber, *Nature* **325**, 419 (1987).
4. D. M. Eigler and E. K. Schweizer, *ibid.* **344**, 524 (1990).
5. M. F. Crommie, C. P. Lutz, D. M. Eigler, *Science* **262**, 218 (1992).
6. H. J. Mamin, P. H. Guethner, D. Rugar, *Phys. Rev. Lett.* **65**, 2418 (1990).
7. H. J. Mamin, S. Chiang, H. Birk, P. H. Guethner, D. Rugar, *J. Vac. Sci. Technol. B* **9**, 1398 (1991).
8. W. Li, J. A. Virtanen, R. M. Penner, *Appl. Phys. Lett.* **60**, 1181 (1992).
9. ———, *J. Phys. Chem.* **96**, 6529 (1992).
10. J. R. LaGraff and A. A. Gewirth, *ibid.* **98**, 11246 (1994).
11. R. Ullmann, T. Will, D. M. Kolb, *Chem. Phys. Lett.* **209**, 238 (1993).
12. ———, *Ber. Bunsenges. Phys. Chem.* **99**, 1414 (1995).
13. The potentials of tip and sample could be controlled independent of each other by means of a bipotentiostat. The tips used for modification and imaging were made from a Pt:Ir wire (80:20) by electrochemical etching and were subsequently coated with Apiezon wax to reduce the area in contact with the electrolyte, thus reducing the faradaic current at the tip to <0.1 nA. The working electrodes were evaporated Au films on Robax AF45 glass (Berliner Glas KG), which, after proper flame-annealing in an H_2-air flame, had (111) surfaces whose quality was similar to that of Au(111) single crystals.
14. R. Gomer, *IBM J. Res. Dev.* **30**, 428 (1986).
15. S. Ciraci, *Springer Ser. Surf. Sci.* **29**, 179 (1993).
16. U. Landman and W. D. Luedtke, *ibid.*, p. 207.
17. L. Kuipers, M. S. Hoogeman, J. W. M. Frenken, *Surf. Sci.* **340**, 231 (1995).
18. N. Batina, T. Will, D. M. Kolb, *Faraday Discuss. Chem. Soc.* **94**, 93 (1992).
19. We are currently examining the possibility of the formation of such structures on semiconducting substrates, which would be of greater technological interest than deposition on metals (D. M. Kolb *et al.*, in preparation).

20. Supported by the Deutsche Forschungsgemeinschaft through grant Ko 576/10-2. We thank R. Liske for developing the microprocessing unit.

3 October 1996; accepted 11 December 1996

Five-Coordinate Hydrogen: Neutron Diffraction Analysis of the Hydrido Cluster Complex $[H_2Rh_{13}(CO)_{24}]^{3-}$

Robert Bau,* Mary H. Drabnis, Luigi Garlaschelli, Wim T. Klooster, Zuowei Xie,† Thomas F. Koetzle,* Secondo Martinengo*

Pentacoordinate hydrogen atoms were identified by single-crystal neutron diffraction analysis of $[N(CH_3)_4]_3[H_2Rh_{13}(CO)_{24}]$. The hydrogen atoms are located in square pyramidal cavities of the Rh_{13} cluster, in positions almost coplanar with the Rh_4 faces on the surface of the cluster. They are slightly displaced inward, toward the central rhodium atom of the cluster, with average H–Rh(central) and H–Rh(surface) distances of 1.84(2) and 1.97(2) angstroms, respectively. This result shows that hydrogen, which normally forms only one bond, can be attached to five other atoms simultaneously in a large metal cluster.

In the late 1970s, it was shown by neutron diffraction (*1*–*3*) that H atoms could exist in the interstitial sites of metal cluster compounds such as $[HCo_6(CO)_{15}]^-$, $[HRu_6(CO)_{18}]^-$, $[HNi_{12}(CO)_{21}]^{3-}$, and $[H_2Ni_{12}(CO)_{21}]^{2-}$. The H atoms were found to be either six-coordinate (μ_6-H), located at the centers of metal octahedra (*1*, *2*), or in triply bridging positions (μ_3-H) on the interior faces of metal octahedral cavities (*3*). Here we report an example of pentacoordinate hydrogen (μ_5-H) found in the square pyramidal cavities of the cluster complex $[H_2Rh_{13}(CO)_{24}]^{3-}$.

The $[H_2Rh_{13}(CO)_{24}]^{3-}$ anion, first reported in 1975 (*4*), is a member of a family of clusters, $[H_xRh_{13}(CO)_{24}]^{(5-x)-}$ (x = 1 to 4), whose members are interconvertible by means of a series of acid-base equilibria (*4*–*9*). The Na salt of the title anion was prepared by refluxing a mixture of $Rh_4(CO)_{12}$ and NaOH in isopropanol under an atmosphere of H_2, followed by addition of Na_2CO_3 (*8*). It was

R. Bau, M. H. Drabnis, Z. Xie, Department of Chemistry, University of Southern California, Los Angeles, CA 90089, USA.
L. Garlaschelli and S. Martinengo, Dipartimento di Chimica Inorganica, Metallorganica e Analytica, Università di Milano, Via G. Venezian 21, Milano 20133, Italy.
W. T. Klooster and T. F. Koetzle, Chemistry Department, Brookhaven National Laboratory, Post Office Box 5000, Upton, NY 11973, USA.
*To whom correspondence should be addressed.
†Present address: Department of Chemistry, Chinese University of Hong Kong, Shatin, Hong Kong.

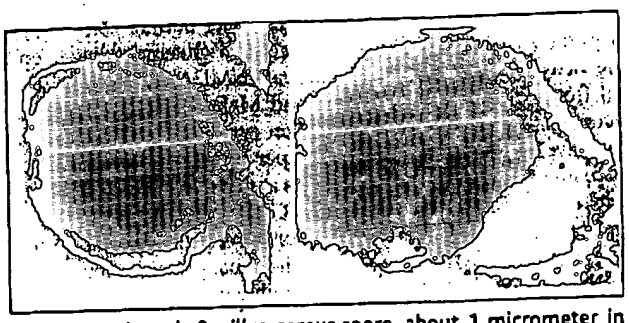

Decommissioned. *Bacillus cereus* spore, about 1 micrometer in diameter, before (left) and 4 hours after exposure to new emulsion.

that kill by rupturing cell membranes. Trial and error led Baker's team to two formulations that demonstrate potent antimicrobial action. An emulsion including the detergents Triton X-100 and tributyl phosphate took out gram-positive bacteria and the vast majority of viruses sheathed in protein envelopes. (Naked RNA viruses are not susceptible, because they have no membrane for the emulsions to disrupt.) A second preparation killed a different spectrum of bugs: gram-negative bacteria and fungi. Combining the armaments yielded a potent killing machine. Exposing a variety of fungi, bacteria, and enveloped viruses to a 1000-fold dilution of the double-barrel emulsion for 15 minutes annihilated the life-forms, the researchers concluded from the absence of colonies in suitable growth media.

To Baker's initial surprise, the emulsions proved effective against bacterial spores—a form of suspended animation in which the bacteria produce a hard protective coat—which tend to resist all but the harshest chemicals. "It appears that the oil acts as a nutrient that tricks the spores to start producing cell membrane, a process that the emulsions disrupt quite easily," said Baker. In one experiment, he and his colleagues infected skin wounds on mice with spores of *Bacillus cereus*, a cause of food poisoning and severe infections. One hour later, the wounds were rinsed with either a 10% solution of the two emulsions or with salt water. The wounds in the treated mice healed, while those in the control animals festered.

Sperm and red blood cells are the only animal cells that Baker's team has found to be susceptible to the emulsions. Other cells are studded with carbohydrates that appear to somehow prevent the emulsion droplets from fusing to the cell membrane. This gentleness is a nice surprise considering that membrane-disrupting antimicrobial peptides have shown unexpected toxicity in animal tissues, says microbiologist Jill Adler Moore, director of the Institute of Cellular and Molecular Biology at California State University in Pomona. The bottom line, says Baker, is that the emulsion mixture is a drug candidate mainly for external uses, such as for treating skin ulcers.

This expectation will soon be put to the test. The National Institute of Child Health and Human Development in Bethesda, Maryland, is planning a clinical trial to see if the emulsions will work as a vaginal contraceptive cream that wards off sexually transmitted diseases. And the U.S. military intends to try to detoxify contaminated equipment by hosing it down with the emulsions, a procedure that could save the equipment from becoming expensive scrap—or paperweights. –JOSEPH ALPER

Joseph Alper is a writer in Louisville, Colorado.

NEUROBIOLOGY

New Clues to How Neurons Strengthen Their Connections

New results point to the AMPA receptor for glutamate as playing a key role in the changes underlying long-term potentiation in brain neurons

Neurobiologists who study how the brain adapts and learns have long known that synapses—the specialized regions where one neuron receives chemical signals from another—are where the action is. For example, learning seems to be associated with an increase in the strength of those synaptic connections. Now, three teams—two of which report their results in this issue of *Science*, while the third published in the May issue of *Nature Neuroscience*—implicate a new player in the biochemical changes underlying a type of synapse strengthening known as long-term potentiation (LTP).

The neurons that undergo LTP respond to the neurotransmitter glutamate. Their synapses contain two kinds of glutamate receptors, but researchers studying LTP have largely focused on the one known as the NMDA receptor. That's because glutamate binding to this receptor is the first step in LTP. Exactly what happens after that is unknown—and the subject of fervent study and debate. The new work fingers the other, less famous glutamate receptor, the AMPA receptor, as a player in those synapse-strengthening events.

Previously, neurobiologists had thought that AMPA receptors are present at relatively unchanging levels in the vast majority of synapses on glutamate-sensitive neurons. But that no longer appears to be the case. Two of the teams, led by Roberto Malinow of Cold Spring Harbor Laboratory on New York's Long Island and Robert Malenka at the University of California, San Francisco, show that AMPA receptors move into and out of synapses as synaptic connections strengthen and weaken. The third team, led by Peter Seeburg and Bert Sakmann of the Max Planck Institute for Medical Research in Heidelberg, Germany, provides indirect evidence that the movements are needed for LTP to occur. Taken together, says Richard Huganir, who studies receptors at Johns Hopkins University School of Medicine in Baltimore, the results give "incontrovertible evidence" that "the regulation of AMPA receptors in general is going to be very key" to modulating synapse strength.

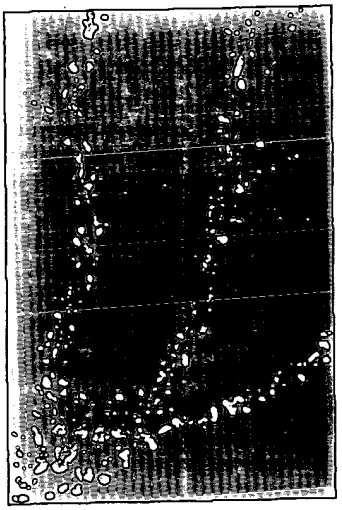

Synaptic togetherness. On these dendritic spines, AMPA receptors are stained green, NMDA receptors are red, and synapses where both are present are yellow.

The current findings are also likely to influence a long-standing debate over whether the changes that occur in LTP take place postsynaptically, that is, in the cell that receives the signal, or presynaptically, in the cell that dispenses it. They imply that at least part of the changes are postsynaptic. Ironically, however, the new findings trace back to an experiment done 9 years ago that was long viewed as strong evidence for presynaptic change.

At that time, the NMDA receptor had already been implicated in LTP, a task for which it is remarkably well suited. Brain neurons usually have thousands of synapses for

CREDITS: (TOP TO BOTTOM) J. GAEB/UNIVERSITY OF MICHIGAN; D. LIAO ET AL., *NATURE NEUROSCIENCE* 2, 37 (1999)